Cellular and Molecular Biology
E-ISSN : 1165-158X / P-ISSN : 0145-5680
www.cellmolbiol.org

Endogenous ligand of the APJ receptor Apelin-13 inhibits cell apoptosis and oxidative stress of cardiomyocytes

Hu Jin[1], Longmeng Cao[1], Dachao Tang[1], Xiaochun Dai[2*]

[1] Department of Cardiovascular Medicine, Wenzhou TCM Hospital of Zhejiang Chinese Medical University, Wenzhou, China
[2] Department of Internal Medicine, The Affiliated Kangning Hospital of Wenzhou Medical University, Zhejiang Provincial Clinical Research Center for Mental Disorder, Wenzhou, China

ARTICLE INFO

Original paper

Article history:
Received: June 25, 2023
Accepted: September 24, 2023
Published: November 15, 2023

Keywords:

Apelin-13, nicotine, H9c2, apoptosis, PI3K/AKT signaling pathway

ABSTRACT

The present study aimed to investigate the effect of Apelin-13 on nicotine-induced injuries of cardiomyocytes. To establish an H9c2 cell model of nicotine-induced apoptosis, H9c2 cells were divided into the control group, nicotine group, and Apelin-13+nicotine group. The apoptosis rate of H9c2 cells was then detected by flow cytometry. Later, the expressions of indicators related to apoptosis, oxidative stress, and inflammatory responses were measured via Western blotting and quantitative real-time polymerase chain reaction (qRT-PCR). The results revealed that the expression of B-cell lymphoma-2 (Bcl-2) was remarkably down-regulated ($P<0.01$), while the apoptosis rate and the expressions of apoptosis-related proteins (Bcl-2-associated X protein (Bax) and cysteinyl aspartate specific proteinase-3 (Caspase-3)) were significantly up-regulated ($P<0.01$) in the nicotine group. However, the variation trends of Bcl-2, Bax, and Caspase-3 in the Apelin-13+nicotine group were contrary to those in the nicotine group ($P<0.01$). Additionally, the expressions of interleukin-1 beta (IL-1β) and tumor necrosis factor-alpha (TNF-α) obviously declined ($P<0.01$), while those of superoxide dismutase 1 (SOD1) and SOD2 dramatically rose in the Apelin-13+nicotine group ($P<0.01$). Furthermore, Apelin-13 treatment evidently elevated the expressions of phosphorylated protein kinase B (p-AKT) and phosphorylated phosphatidylinositol 3-kinase (PI3K). In conclusion, Apelin-13 inhibits nicotine-induced apoptosis and oxidative stress in H9c2 cells *via* the PI3K/AKT signaling pathway.

Doi: http://dx.doi.org/10.14715/cmb/2023.69.11.31

Introduction

In recent years, the morbidity and mortality of cardiovascular diseases have been ranked first in the world. According to epidemiological studies, smoking is a major risk factor for cardiovascular events (1).

Nicotine, a key ingredient in cigarettes, is one of the contributors to cardiovascular disease and respiratory diseases (2). Related studies have shown that nicotine can trigger cardiomyocyte apoptosis (3), and cardiomyocyte apoptosis has been recognized as the mechanism underlying the development of cardiomyopathy and heart failure (4). It has also been demonstrated by in vitro studies that nicotine can cause myocardial cell dysfunction, accompanied by significant interstitial fibrosis (5). In recent years, numerous studies have shown that nicotine aggravates the inflammatory response in myocardial injury, oxidative stress, apoptosis, and myocardial fibrosis (6). However, the mechanism underlying nicotine-induced injuries of cardiomyocytes remains unclear.

Apelin-13, an endogenous ligand of the Apelin receptor (APJ), is highly expressed in the heart. The Apelin/APJ system plays a crucial regulatory role in the pathophysiology of cardiovascular diseases, and the Apelin/APJ axis can be a novel therapeutic target for cardiovascular diseases (7). As reported, Apelin-13 exerts vasodilatory and antihypertensive effects, so it can be used to regulate blood pressure (8). In addition, there is evidence that exogenous Apelin-13 can ameliorate cardiac dysfunction and remodeling in rats with heart failure (9).

The phosphatidylinositol-3-kinase (PI3K) pathway is involved in the regulation of cardiovascular diseases (10). PI3Ks are phosphorylated upon receptor tyrosine kinase-dependent activation, and the intensity of PI3K activation is regulated by phosphatase and tensin homolog deleted on chromosome ten (PTEN). PDK1, a key element of signal transduction, activates the protein kinase B (AKT), and the activated AKT then regulates the activation of downstream effector molecules, including mammalian target of rapamycin (mTOR) and subsequent P70S6K, as well as other targets such as GSK3, WEE1 or BAD (11). In addition, the PI3K pathway regulates cellular activities such as protein synthesis, cell cycle, and apoptosis. PI3Ks are composed of a heterodimer between a p110 catalytic subunit and a p85 regulatory subunit (12). Recent studies have manifested that the Apelin/APJ system regulates the cardiomyocyte cycle by interacting with different pathways, including the PI3K/AKT signaling pathway, the cysteinyl aspartate specific proteinase-3 (Caspase-3) pathway, and the autophagy pathway (13). In this study, therefore, the effects of Apelin-13 on nicotine-induced injuries of H9c2 cells and the underlying molecular mechanism were investigated.

* Corresponding author. Email: 419129558@qq.com

Materials and Methods

Cell culture

The H9c2 cell line was purchased from the Cell Bank of the Chinese Academy of Sciences (Shanghai, China), and routinely cultured in Dulbecco's Modified Eagle's Medium (DMEM; Life Technology, Wuhan, China) containing 10% fetal bovine serum (FBS; Life Technology, Wuhan, China) and 1% streptomycin in a cell culture incubator.

Cell grouping

Apelin-13 and nicotine were bought from Sigma (St. Louis, MO, USA).To explore the effect of Apelin-13 on nicotine-induced apoptosis, H9c2 cells were divided into the control group, nicotine group, and Apelin-13+nicotine group.

Drug treatment

H9c2 cells in the logarithmic growth phase were treated with drugs until cell confluence reached about 60%. Then the cells were pre-incubated with Apelin-13 (100 μmol/L) for 2 h and stimulated by nicotine (10 μmol/L) for 48 h. The concentration was determined according to the method described in a previous report [14].

Cell Counting Kit-8 (CCK-8) assay

A CCK-8 () assay was performed to measure the viability of H9c2 cells in different groups according to the kit instructions. Specifically, H9c2 cells in the logarithmic phase were inoculated into 96-well plates at a density of 5×10^3/well and cultured with different concentrations of Apelin-13 added into the plates. The next day, the stop solution (Nanjing Jiancheng Bioengineering Institute, Nanjing, China) was added to each group at 1 h, 2 h, 4 h, and 8 h, respectively. Finally, the optical density (OD) of each well was measured at a wavelength of 450 nm.

Western blotting assay

H9c2 cells in the logarithmic growth phase were treated with drugs until about 60% confluence. After 24 h, the cells were collected and lysed. Next, the total protein was extracted, and its concentration was determined by a bicinchoninic acid (BCA) assay (Pierce, Rockford, IL, USA). The extracted proteins (20 μg) were separated on 10% sodium dodecyl sulfate-polyacrylamide gel electrophoresis (SDS-PAGE) gels and subsequently transferred to a polyvinylidene difluoride membrane (Millipore, Billerica, MA, USA). Later, the membranes were incubated with antibodies against superoxide dismutase 1 (SOD1) (1:3000), SOD2 (1:3000), B-cell lymphoma-2 (Bcl-2) (1:2000), Bcl-2-associated X protein (Bax) (1:2000), Caspase-3 (1:3000), interleukin-1 beta (IL-1β) (1:5000), tumor necrosis factor-alpha (TNF-α) (1:500), PI3K (1:500), phosphorylated (p)-PI3K (1:1000), AKT (1:2000), p-AKT (1:2000), and glyceraldehyde-3-phosphate dehydrogenase (GAPDH) (1:5000) (Abcam, Cambridge, MA, USA) overnight at 4°C. After routine washing, the membranes were incubated with secondary antibodies. The ratio of $OD_{(\text{target bands})}/OD_{(\text{internal reference bands})}$ was analyzed in a gel image processing system. Lastly, a grayscale analysis was performed using ImageJ and a statistical analysis was performed on Prism.

Quantitative real-time polymerase chain reaction (qRT-PCR)

The total RNA was extracted from each group of cells by TRIzol reagent (Sigma, St. Louis, MO, USA). Next, complementary deoxyribose nucleic acid (cDNA) was reversely transcribed using the PrimeScript RT reagent kit (Takara Biotechnology Co., Ltd., Dalian, China). The PCR amplification conditions were set as follows: 38 cycles of denaturation at 95°C for 5 min, at 95°C for 5 s, at 60°C for 35 s, and at 72°C for 20 s, followed by extension at 72°C for 5 min. The expression level of target genes was calculated by the $2^{-\Delta\Delta Ct}$ method. Primers were designed using Primer 6.0 software, which are listed in Table 1.

Enzyme-linked immunosorbent assay (ELISA)

After counting, H9c2 cells were seeded into 12-well plates at 10/well and received different treatments in the three groups. Later, the supernatants were collected, and the corresponding indicators were detected by an ELISA kit (Elabscience, Wuhan, China).

SOD concentration detection

H9c2 cells were counted, and an equal number of cells were cultured in a culture dish. After separate treatment in each group, the cells were lysed using a lysis buffer, and the protein concentration was detected using a BCA kit. Following the same multiple dilution, the SOD concentration was examined using the SOD assay kit (Elabscience, Wuhan, China), and the OD value was determined.

Lactate dehydrogenase (LDH) concentration detection

In each group, the supernatant was collected, and the LDH concentration was measured according to the instructions of the LDH assay kit (Elabscience, Wuhan, China).

Immunofluorescence

H9c2 cell slides seeded in 24-well plates were washed

Table 1. RT-PCR primers.

Gene name	Forward (5'>3')	Reverse (5'>3')
Bax	TGAAGACAGGGGCCTTTTTG	AATTCGCCGGAGACACTCG
Bcl-2	GTCGCTACCGTCGTGACTTC	CAGACATGCACCTACCCAGC
GPX1	ATCATATGTGTGCTGCTCGGCTAGC	TACTCGAGGGCACAGCTGGGCCCTTGAG
GPX2	GCCTCAAGTATGTCCGACCTG	GGAGAACGGGTCATCATAAGGG
Caspase-3	ATGGAGAACAACAAAACCTCAGT	TTGCTCCCATGTATGGTCTTTAC
PI3K	ACTCTCTCTTCTTCCTTTTCCTCTA	CTAAACTTTTTCCCACCACCTA
AKT	TCATTCTACTCCTCACCTTCCAT	CTCCTCTCCCTTTTGAGTCCAT
IL-1β	GCAACTGTTCCTGAACTCAACT	ATCTTTTGGGGTCCGTCAACT
TNF-α	CCTCTCTCTAATCAGCCCTCTG	GAGGACCTGGGAGTAGATGAG
GAPDH	ACAACTTTGGTATCGTGGAAGG	GCCATCACGCCACAGTTTC

RT-PCR: real-time polymerase chain reaction.

with phosphate-buffered saline (PBS) and fixed with methanol. After washing with PBS again, goat serum was added for blocking at room temperature for 30 min, and the slides were incubated with fluorescent primary antibodies against SOD1 (Abcam, rabbit, 1:3000) and IL-1β (Abcam, rabbit, 1:3000) overnight at 4°C. Afterward, the slides were further incubated with fluorescent secondary antibodies for 1 h at 37°C in the dark and then washed with PBS. Later, the cells were stained with 4',6-diamidino-2-phenylindole (DAPI) for 5-10 min, and an anti-extractor was added dropwise. The results were observed under a fluorescence microscope.

Immunochemistry

H9c2 cell slides inoculated in 24-well plates were washed with PBS and fixed with methanol. After washing with PBS again, 5% goat serum was added for 30 min of blocking at 37°C, and the slides were incubated with the primary antibodies against Caspase-3 (Abcam, Rabbit, 1:1000) overnight at 4°C. The next day, the slides were washed with PBS and incubated with the secondary antibodies at room temperature for 1 h. Next, 3,3'-diaminobenzidine (DAB) was used for color development, and the slides were observed under the microscope, fully washed, and finally dehydrated.

Apoptosis analysis via flow cytometry

H9c2 cells in the logarithmic growth phase were treated with drugs until cell confluence of about 60%. After collection and counting (density: 5×10^8/L), the cells were washed twice with pre-cooled PBS. Then the supernatant was sucked out, and the cells were resuspended with 100 μL of binding buffer and transferred to 1.5 mL Eppendorf (EP) tubes. Subsequently, the cells in each EP tube were incubated with Annexin V-FITC (KeyGEN BioTECH, Nanjing, China) and propidium iodide at room temperature in the dark, and an apoptosis analysis was conducted using a flow cytometer (Becton Dickinson, Heidelberg, Germany).

Intracellular reactive oxygen species (ROS) level

The differently-treated H9c2 cells were collected and washed with pre-cooled PBS. After loading with the probe DCFH-DA (10 M, KeyGEN BioTECH, Nanjing, China), the remaining probes that did not enter the cells were washed, and the total ROS level was detected using the flow cytometer (Becton Dickinson, Heidelberg, Germany).

Statistical analysis

Statistical Product and Service Solutions (SPSS) 22.0 (IBM, Armonk, NY, USA) software was adopted for statistical analysis. The data were compared among multiple groups using a one-way analysis of variance (ANOVA), followed by a post hoc test (least significant difference). $P<0.05$ represented that the difference was statistically significant.

Results

Apelin-13 inhibited nicotine-induced apoptosis of H9c2 cells

CCK-8 results showed that the optimal concentration of Apelin-13 was 100 μmol/L, at which Apelin -13 exerted a significant effect on nicotine-induced apoptosis, and the viability of H9c2 cells was the highest at 2 h (Figure 1A). In addition, the nicotine group had dramatically higher expressions of Bax and Caspase-3 and a lower Bcl-2 expression than the control group. The variation trends of the expressions of Bax, Caspase-3, and Bcl-2 in the Apelin-13+nicotine group were obviously opposite to those in the nicotine group (Figure 1B-1C). According to the qRT-PCR results, the mRNA expressions were similar in the three groups (Figure 1D-1F). In addition, the apoptosis rate of H9c2 cells obviously rose in the nicotine group but significantly declined in the Apelin-13+nicotine group (Figure 1G). At the same time, as revealed by immunocytochemistry results, Apelin-13 attenuated the nicotine-induced increase of Caspase-3 (Figure 1H).

Apelin-13 inhibited nicotine-induced oxidative stress in H9c2 cells

Firstly, the expressions of SOD1 and SOD2 were examined by Western blotting (Figure 2A-2B). It was found that in the nicotine group, the antioxidant capacity was obviously down-regulated, and the expressions of SOD1 and SOD2 were evidently reduced, which could be effectively alleviated by Apelin-13. Secondly, the mRNA expressions of glutathione peroxidase 1 (GPX1) and GPX2 were also significantly elevated in the Apelin-13+nicotine group (Figure 2C-2D). In addition, the protein expressions of SOD1 and SOD2 were in line with the SOD concentration detection results (Figure 2E). However, the LDH was markedly up-regulated in the nicotine group but notably down-regulated in the Apelin-13+nicotine group (Figure 2F). Furthermore, the flow cytometry results also confirmed that nicotine-induced oxidative stress in H9c2 cells (Figure 2G), and the immunofluorescence detection results

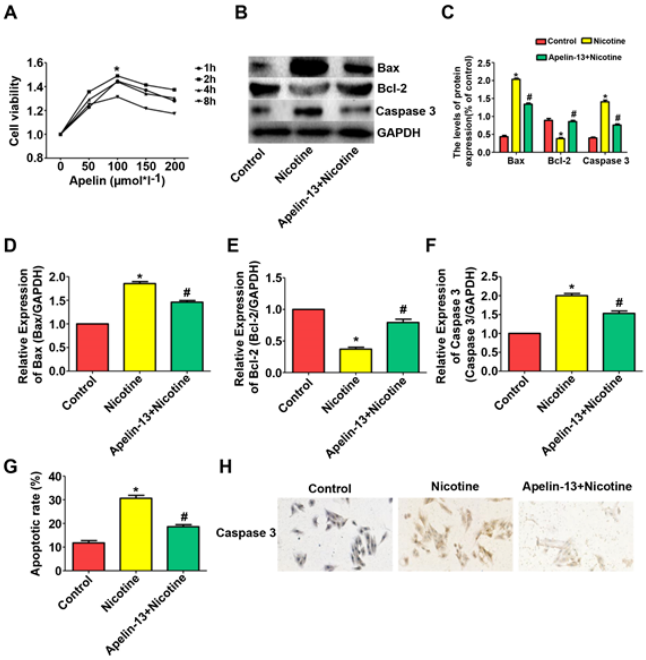

Figure 1. Apelin-13 inhibits nicotine-induced apoptosis of H9c2 cells. (A) The optimal concentration of Apelin-13 and time points were detected *via* CCK-8 assay. (B-C) The protein expressions of Bax, Bcl-2, and Caspase-3 were detected by Western blotting assay. (D-F) The mRNA expressions of Bax, Bcl-2, and Caspase-3 were detected by qRT-PCR. (G) The apoptosis rate of H9c2 cells. (H) Caspase-3 expression detected by immunocytochemistry (100×). $^*P<0.05$ *vs.* the control group, and $^\#P<0.05$ *vs.* the nicotine group.

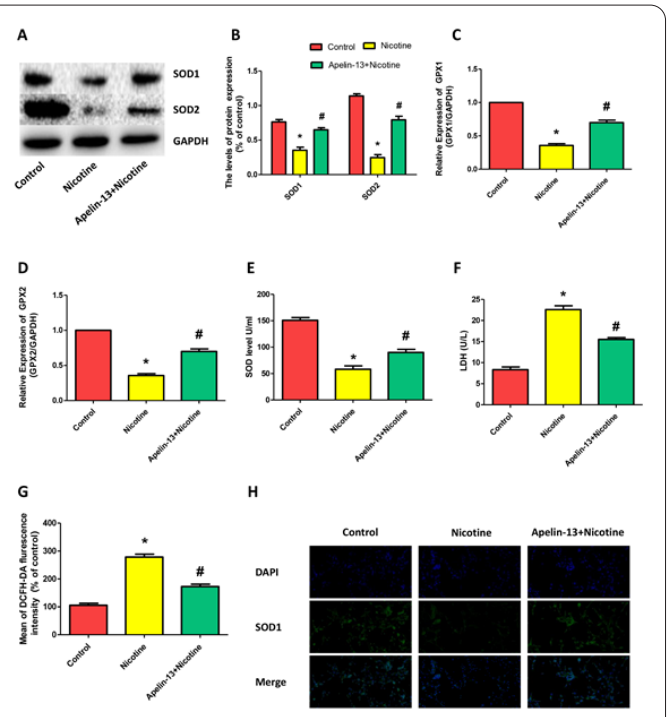

Figure 2. Apelin-13 inhibits nicotine-induced oxidative stress in H9c2 cells. (A-B) The protein expressions of SOD1 and SOD2 were examined by the Western blotting assay. (C-D) The mRNA expressions of GPX1 and GPX2. (E) SOD concentration detection results. (F) LDH concentration detection results. (G) ROS level detection results. (H) SOD1 expression detected by immunofluorescence (400×). $^{*}P<0.05$ *vs.* the control group, and $^{\#}P<0.05$ *vs.* the nicotine group.

manifested that Apelin-13 partially reversed the nicotine-induced decline in the SOD1 expression (Figure 2H).

Apelin-13 suppressed nicotine-induced inflammatory responses in H9c2 cells

There is evidence that apoptosis and oxidative stress are associated with inflammatory responses. Therefore, the corresponding inflammatory cytokines were also detected in this study. The results showed that nicotine-induced inflammatory responses in cells. The protein expressions of IL-1β and TNF-α were dramatically raised in the nicotine group but markedly reduced in the Apelin-13+nicotine group (Figure 3A-3B). At the same time, the mRNA expressions of IL-1β and TNF-α were consistent with the results of protein expressions (Figure 3C-3D). Moreover, ELISA results revealed that the levels of IL-1β and TNF-α were similar (Figure 3E-3F), and immunofluorescence detection results also demonstrated that Apelin-13 effectively inhibited the nicotine-induced increase in the IL-1β expression (Figure 3G).

Apelin-13 might activate the PI3K/AKT signaling pathway

Next, attempts were made to explore the molecular mechanism by which Apelin-13 inhibits nicotine-induced apoptosis and oxidative stress in H9c2 cells. Through literature review and analyses based on multiple databases, it was speculated that the PI3K/AKT signaling pathway may be involved in the molecular mechanism. Interestingly, as speculated, the protein expressions of p-AKT and p-PI3K in the nicotine group evidently dropped compared with those in the control group, while the total protein expressions of AKT and PI3K displayed no remarkable changes. Additionally, the protein expressions of p-AKT

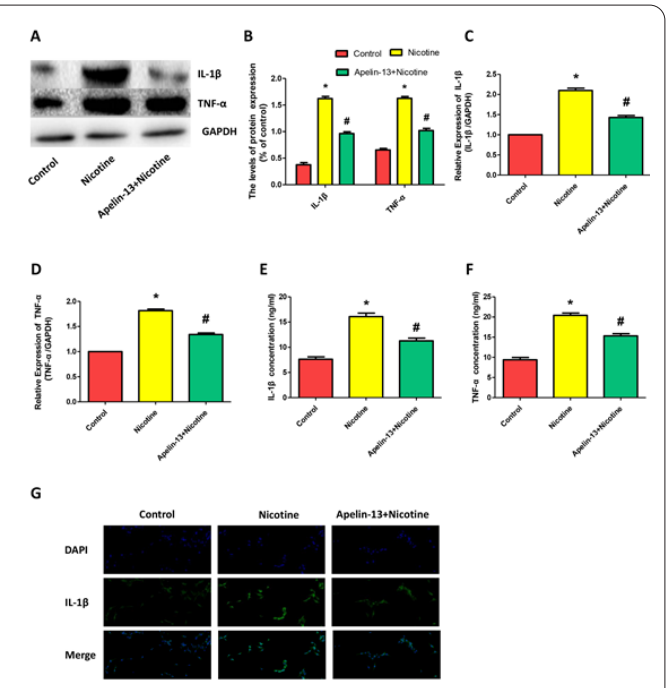

Figure 3. Apelin-13 inhibits nicotine-induced inflammatory responses in H9c2 cells. (A) The protein expressions of IL-1β and TNF-α detected *via* the Western blotting assay. (C-D) The mRNA expressions of IL-1β and TNF-α. (E-F) IL-1β and TNF-α concentrations were detected *via* the ELISA. (G) IL-1β expression measured by immunofluorescence (400×). $^{*}P<0.05$ *vs.* the control group, and $^{\#}P<0.05$ *vs.* the nicotine group.

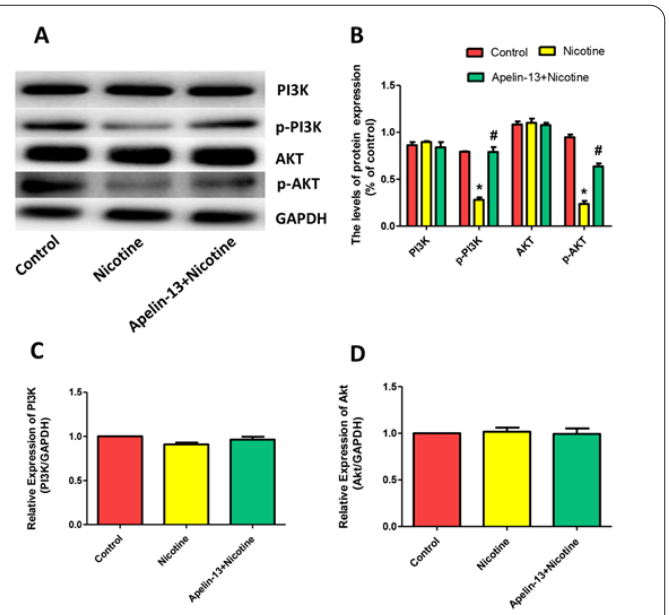

Figure 4. Apelin-13 may activate the PI3K/AKT signaling pathway. (A) The protein expressions of PI3K, AKT, p-PI3K, and p-AKT were examined by the Western blotting assay. (C-D) The mRNA expressions of PI3K and AKT. $^{*}P<0.05$ *vs.* the control group, and $^{\#}P<0.05$ *vs.* the nicotine group.

and p-PI3K markedly rose in the Apelin-13+nicotine group (Figure 4A- 4B), which were similar to the results of qRT-PCR (Figure 4C-4D). Taken together, Apelin-13 might activate the PI3K/AKT signaling pathway.

Discussion

Correcting risk factors is a good strategy to reduce the burden of cardiovascular diseases, which kills more than

16 million people worldwide each year (15). According to the literature, smoking is a risk factor for many cardiovascular diseases and is one of the main causes of premature death among smokers. The latest reports show that smokers display a loss of life expectancy by at least 10 years compared with people who never smoked. However, preventive or therapeutic measures for cardiovascular toxicity associated with cigarette smoking have rarely been reported (16).

Apelin-13 is an endogenous ligand for the APJ and a member of the G protein-coupled receptor family, which is highly expressed in the heart (17). When cardiomyocytes are exposed to nicotine or stimulated by cigarette smoking mitochondrial metabolism and function will be changed, which activates the mitochondria-mediated intrinsic apoptotic pathways, thereby triggering mitochondrial dysfunction and changes in apoptosis-related proteins, including Bax and Bcl-2, and ultimately activating cytochromes C and Caspase, especially Caspase-3. This finding indicates that these apoptosis-related proteins play crucial roles in cell damage and apoptosis (18). In addition, previous evidence has demonstrated inflammatory responses are correlated with oxidative stress and apoptosis (19).

In this study, H9c2 cells were used to establish a cardiomyocyte model of nicotine-induced apoptosis *in vitro*. The experimental results revealed that the expressions of Caspase-3 and Bax were obviously up-regulated but Bcl-2 expression was dramatically inhibited in H9c2 cells exposed to nicotine. At the same time, the oxidative stress was activated, causing mitochondrial dysfunction, which elevated the level of intracellular ROS and led to redox imbalance. According to the CCK-8 assay results, the effects of different concentrations of Apelin-13 on the nicotine-induced apoptosis of H9c2 cells largely varied, and Apelin-13 itself did not have toxic effects on H9c2 cells. Therefore, the concentration of Apelin-13 used in the subsequent experiment was 100 μmol/L. It was also uncovered that the protein expressions of p-PI3K and p-AKT were markedly down-regulated in H9c2 cells exposed to nicotine, but they were obviously up-regulated in the cells pre-incubated with Apelin-13 (Figure 5). Related reports have shown that the PI3K/AKT pathway plays a critical role in cellular functions such as cell apoptosis, and it mediates various growth factors to regulate cellular functions by phosphorylating or inhibiting its downstream targets, thereby exerting the regulatory effects of these factors on growth, apoptosis, and survival (20-22). The above findings are consistent with the results of this study.

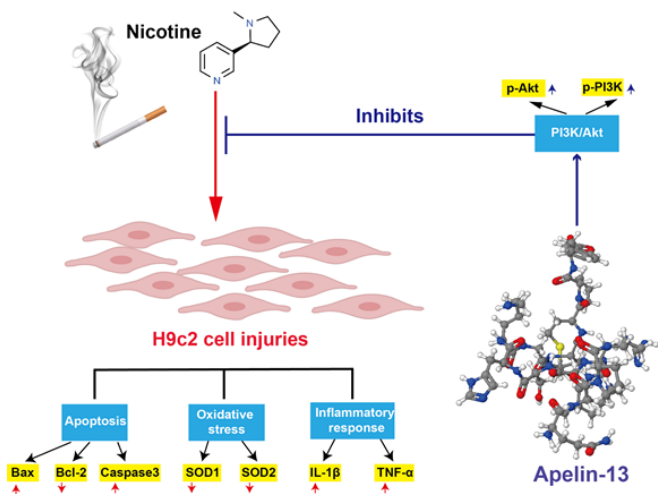

Figure 5. A schematic map illustrates that Apelin-13 activates the PI3K/AKT signaling pathway, thus inhibiting nicotine-induced apoptosis, inflammatory responses, and oxidative stress in H9c2 cells.

Innovatively, this study explores the molecular mechanism by which Apelin-13 attenuates nicotine-induced injuries of cardiomyocytes, which provides a molecular basis for drug intervention in the treatment of cardiovascular diseases in the future. However, there are still several obvious limitations in the present study. For example, the results of this study have not been validated in animal models. In future experiments, attempts will be made to establish animal models of nicotine-induced myocardial injury to further explore whether Apelin-13 can alleviate nicotine-induced cell apoptosis and oxidative stress and to investigate the underlying mechanism.

This study demonstrates that Apelin-13 inhibits nicotine-induced H9c2 cell apoptosis and oxidative stress through the PI3K/AKT signaling pathway, thus reducing inflammation and delaying cellular senescence.

Data availability

The datasets used and analyzed during the current study are available from the corresponding author upon reasonable request.

Acknowledgments

Not applicable.

Funding

This study was supported by the Wenzhou Science and Technology Bureau Project (Y2020300).

Conflict of interest

The authors declare that they have no competing interests.

References

1. Mainali P, Pant S, Rodriguez AP, Deshmukh A, Mehta JL. Tobacco and cardiovascular health. Cardiovasc Toxicol 2015; 15(2): 107-116.
2. Gallucci G, Tartarone A, Lerose R, Lalinga AV, Capobianco AM. Cardiovascular risk of smoking and benefits of smoking cessation. J Thorac Dis 2020; 12(7): 3866-3876.
3. Meng TT, Wang W, Meng FL, et al. Nicotine Causes Mitochondrial Dynamics Imbalance and Apoptosis Through ROS Mediated Mitophagy Impairment in Cardiomyocytes. Front Physiol 2021; 12: 650055.
4. Xin LH, Liu WJ, Song T, Zhang L. Overexpression of DJ-1 expression protects cardiomyocyte apoptosis induced by ischemia reperfusion. Eur Rev Med Pharmaco 2020; 24(23): 11988.
5. Hu N, Guo R, Han X, Zhu B, Ren J. Cardiac-specific overexpression of metallothionein rescues nicotine-induced cardiac contractile dysfunction and interstitial fibrosis. Toxicol Lett 2011; 202(1): 8-14.
6. Zhou X, Sheng Y, Yang R, Kong X. Nicotine promotes cardiomyocyte apoptosis via oxidative stress and altered apoptosis-related gene expression. Cardiology 2010; 115(4): 243-250.
7. Yamaleyeva LM, Shaltout HA, Varagic J. Apelin-13 in blood pressure regulation and cardiovascular disease. Curr Opin Nephrol Hy 2016; 25(5): 396-403.
8. Han X, Zhang DL, Yin DX, Zhang QD, Liu WH. Apelin-13 deteriorates hypertension in rats after damage of the vascular endothelium by ADMA. Can J Physiol Pharm 2013; 91(9): 708-714.

9. Koguchi W, Kobayashi N, Takeshima H, Ishikawa M, Sugiyama F, Ishimitsu T. Cardioprotective effect of apelin-13 on cardiac performance and remodeling in end-stage heart failure. Circ J 2012; 76(1): 137-144.
10. Su D, Zhou Y, Hu S, et al. Role of GAB1/PI3K/AKT signaling high glucose-induced cardiomyocyte apoptosis. Biomed Pharmacother 2017; 93: 1197-1204.
11. Ersahin T, Tuncbag N, Cetin-Atalay R. The PI3K/AKT/mTOR interactive pathway. Mol Biosyst 2015; 11(7): 1946-1954.
12. Qin W, Cao L, Massey IY. Role of PI3K/Akt signaling pathway in cardiac fibrosis. Mol Cell Biochem 2021; 476(11): 4045-4059.
13. Xie F, Liu W, Feng F, et al. Apelin-13 promotes cardiomyocyte hypertrophy via PI3K-Akt-ERK1/2-p70S6K and PI3K-induced autophagy. Acta Bioch Bioph Sin 2015; 47(12): 969-980.
14. Huang C, Guo X, Zhao H, et al. Nicotine induces H9C2 cell apoptosis via Akt protein degradation. Mol Med Rep 2017; 16(5): 6269-6275.
15. Montanaro C. Cardiovascular risk in adolescents. Int J Cardiol 2017; 240: 444-445.
16. Banks E, Joshy G, Korda RJ, et al. Tobacco smoking and risk of 36 cardiovascular disease subtypes: fatal and non-fatal outcomes in a large prospective Australian study. Bmc Med 2019; 17(1): 128.
17. Sekerci R, Acar N, Tepekoy F, Ustunel I, Keles-Celik N. Apelin/APJ expression in the heart and kidneys of hypertensive rats. Acta Histochem 2018; 120(3): 196-204.
18. Liao HE, Lai CH, Ho TJ, et al. Cardio Protective Effects of Lumbrokinase and Dilong on Second-Hand Smoke-Induced Apoptotic Signaling in the Heart of a Rat Model. Chinese J Physiol 2015; 58(3): 188-196.
19. Niewiarowska-Sendo A, Kozik A, Guevara-Lora I. Influence of bradykinin B2 receptor and dopamine D2 receptor on the oxidative stress, inflammatory response, and apoptotic process in human endothelial cells. Plos One 2018; 13(11): e206443.
20. Kakaei M, Rehman FU, Fazeli F. The effect of chickpeas metabolites on human diseases and the application of their valuable nutritional compounds suitable for human consumption. Cell Mol Biomed Rep 2024; 4(1): 30-42. doi: 10.55705/cmbr.2023.395591.1153.
21. Reddy PR, Poojitha G, Kavitha S, Samreen SL, Naseer A, Koteswari P, Soumya P. A prospective observational study to assess the cardiac risk factors and treatment patterns in established heart diseases. Cell Mol Biomed Rep 2022;2(4):265-75. doi: 10.55705/cmbr.2022.362447.1067.
22. Li Y, Ruan X, Chen T, Gao J, Wang X. Anti-apoptotic effect of Suxiao Jiuxin Pills against hypoxia-induced injury through PI3K/Akt/GSK3beta pathway in HL-1 cardiomyocytes. J Chin Med Assoc 2018; 81(9): 816-824.